Modeling the Conductance of Single-Molecule Electron Transport in a Symmetric Break Junction

Kevin Hoxha

Half Hollow Hills High School East

I. Abstract

A break junction is an electronic device that consists of two electrodes separated by a very thin gap in the order of a few nanometers. Electron transport through an Oligo(phenylene ethynylene)dithiol (OPE3) molecule in a mechanically-controlled break junction with gold electrodes through a potential difference of 100 mV was measured with 41916 trials. The data was separated into 3 classes corresponding to different channels through which electrons could flow. Class 1 represented quantum tunneling through the electrodes, Class 2 represented single-molecule transport through the benzene rings of the OPE3 molecule, and Class 3 represented single-molecule transport through Au-S bonds in the molecule. A probability density function was constructed to model non-resonant symmetric tunneling based on the assumption that coupling strengths between the channels and electrodes, as well as the channel energies, are normally distributed. A Python program was developed to find the best fit line for the experimental data collected from the OPE3 molecule. Molecule's channel energy and coupling strengths were extracted from the model. All prominent channels are well-described by the model, and the inclusion of the background tunneling is necessary to eliminate a fitting error of approximately 25%. OPE3 is used in polymer form in carbon-based photovoltaics, so understanding how electrons flow through the molecule is critical in designing more efficient solar cells.

II. Introduction

In the field of nano-physics, the study of electron transport is concerned with the flow of electrons through nanoscale systems. Typically, these systems consists of a single molecule. This field of study has become an active research topic as we seek to understand the fundamental quantum effects that govern all phenomena at such a small scale [22]. Additionally, electron transport knowledge is currently utilized in several applications in spectroscopy, molecular transistors, photovoltaics, superconductivity, and hypersensitive detectors [36]. Regardless of motivations, understanding the flow of electricity through single-molecule systems is challenging both in terms of carrying out reliable and reproducible experiments, as well as developing solid theoretical models to explain it.

Break Junctions

The most common way of measuring the physical properties of molecules and their ability to act as conductors of electricity is to place them in break junctions. A break junction is an electronic device consisting of two electrodes separated by a very thin gap in the order of a few nanometers. A potential difference is applied to the two electrodes and the detection of any electric current is the proof that electrons were able to be transported through the molecules that filled the gap [25]. Using an ammeter, the current can be measured and Ohm's Law can be employed to calculate the conductance of the molecule. Experiments have shown that there is some electrical current across the electrodes even when the gap is too small to be filled by a molecule, thus hinting to quantum tunnelling being the cause of such non-zero conductance observations. A break junction can be created in multiple ways, including physically pulling electrodes apart, chemical etching, and electromigration. The most common way for a break

junction to be created is through a mechanically-controlled break junction [30]. With this method, a solid piece of metal is bent using a machine until a fracture is created. The electric current is continuously measured as the fractured pieces of the metal are pulled apart and molecules being studied fall inside the gap and electron transport begins.

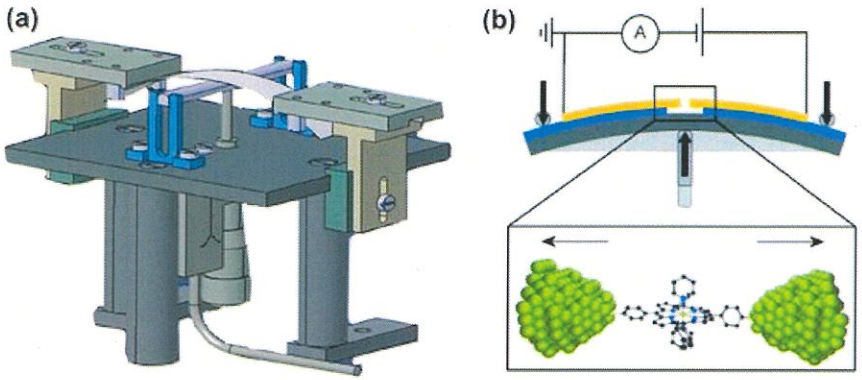

Figure 1: Diagram of a mechanically-controlled break junction. A plate of gold is slowly split, and then connected to a potential difference. A single molecule is placed between gold electrodes. Source: Adapted from Perrin et al.

A break junction can be filled by either a single molecule or multiple ones. The molecules will also fall into the gap in different, random orientations, thus giving rise to many patterns of conductivity that are intrinsically stochastic. Conductance measurements from a single-molecule break junction describe the electronic properties of the molecule being studied. These conductance measurements are difficult to reproduce and, as a result, a large number of experiments is done to collect a large data set to be used for further analysis. In order to avoid the effects of thermal energy, the break junction experiments are often performed in ultra-high vacuum and low temperatures of about 4-5K.

Conductance Histograms

A conductance histogram is a compilation of conductance measurements from a break junction. It depicts the relationship between the number of times a conductance G is measured

versus the value of G. Effectively, these histograms are the probability density function for measuring a particular conductance range. The peak of a conductance histogram is the accepted conductance value of the molecule studied. Conductance values are measured in multiple of $G_0 = 2e^2/h$, which is known as the conductance quantum, where e is the charge of an electron and h is Planck's constant. G_0 represents the conductance value through a single molecule just before the electrodes are fractured and conductance drops [36]. Conductance histograms are used to depict conductance measurements because of the large amount of measurements due to the stochastic nature of break junctions. Using a conductance histogram allows the viewer to easily understand the most common conductance value.

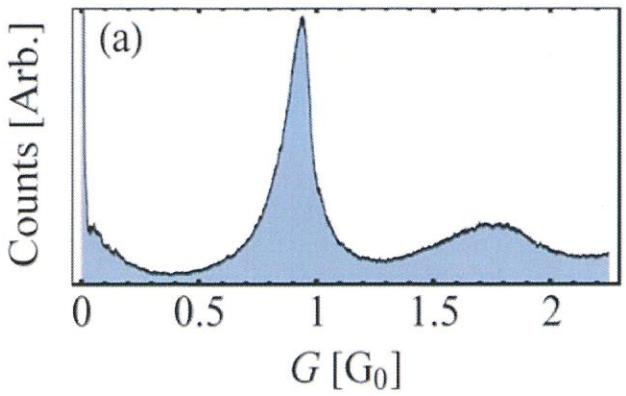

Figure 2: Conductance histogram which represents electron transport through a single gold molecule in a symmetric break junction with gold electrodes. Accepted conductance value is approximately 1 G_0. Source: Adapted from Reuter et al.

Symmetric Nonresonant Model

The Landauer-Büttiker function states:

$$T_{\text{molecule}}(E) = \frac{4\Gamma_L\Gamma_R}{4(E-\varepsilon)^2 + (\Gamma_L+\Gamma_R)^2}$$

where Γ_L and Γ_R represent the coupling strengths between channels and their respective electrodes, ε represents the channel energy, and T(E) represents the probability that a channel

transmit an electron of energy E [5]. A break junction could have asymmetrical electrodes, which would mean that Γ_L does not equal Γ_R.

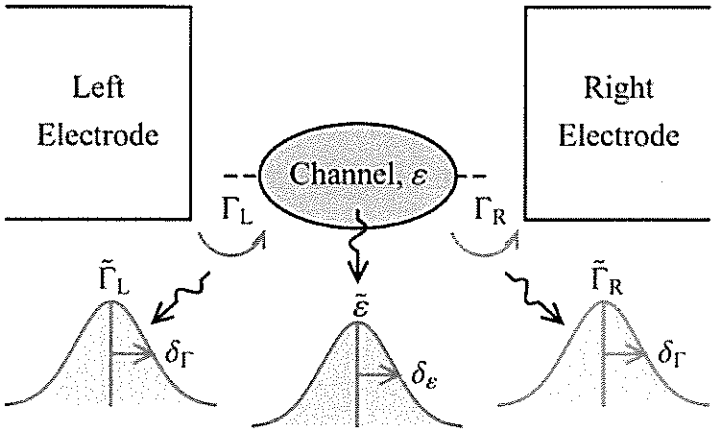

Figure 3: Through a given channel, the channel energy, ε, and coupling strengths, Γ_L and Γ_R, will be normally distributed. Source: Adapted from Williams et al.

In a symmetric nonresonant model, the left electrode is identical to the right electrode. This allows us to assume that $\Gamma_L = \Gamma_R$ and $4(E-\varepsilon)^2$ is much greater than $(\Gamma_L+\Gamma_R)^2$. Also, we must assume that both coupling strengths and the channel energy are normally distributed. By following these assumptions, we can simplify the Landauer-Büttiker function to:

$$T_{NR}(E) \approx \frac{\Gamma^2}{(E-\varepsilon)^2}$$

Using this simplified form will allow us to more easily create a mathematical model which matches experimental data produced by a mechanically-controlled break junction [22].

III. Objectives

The ultimate goal of my research is for my results to be used as foundational knowledge for experimentalists to develop more efficient carbon-based photovoltaics. To gain a better understanding of electron transport through a single molecule break junction, I will create

computational models which explain experimental results through a symmetric single-molecule break junction with gold electrodes travelling through oligo(phenylene ethynylene)dithiol (OPE3). I also will take into account the effects of background tunneling in my model to create a more accurate approximation for the experimental data. This model should explain data not only from this molecule, but for all other break junctions. The experimental data will also be divided by a machine learning algorithm, which aims to describe each of the paths an electron could take to travel through a break junction. If the model fits the unfiltered data as well as each channel, then it confirms that each channel acts independently and that the machine learning algorithm correctly divides the data into proper classes. To achieve these goals, the following objectives are set:

i. Investigate the processes by which electric currents flow through a single molecule connected between two electrodes.

ii. Develop theoretical and computational models to explain experimental conductance histograms for electron transport through single-molecule break junctions.

iii. Extract molecular properties and other insights from experimental datasets.

IV. Methodology

Break Junction Experiments

My research aims to fit a mathematical and computational model to experimental data and, without experimental data to test it on, it would be worthless. My collaborators based in The Netherlands, including Damien Cabosart, Maria El Abbassi, Herre S.J. van der Zant, Mickael L. Perrin, and others, have allowed us to use their experimental data to test our mathematical model.

In their experimental setup, a mechanically-controlled break junction with gold electrodes was set up in a symmetric nonresonant model. A single Oligo (phenylene ethynylene) dithiol (OPE3) molecule was placed in the gap in the break junction. 41916 measurements were taken in order to create a vast data set for the stochastic break junction. A potential difference of 100 mV was developed across the break junction in order for electron transport to be facilitated.

Figure 4: The structure of an OPE3 molecule. Benzene rings are found in the middle with gold and sulfur bonds on the outside of the organic molecule. Source: Student generated image

Machine Learning Algorithm

Machine learning techniques were also used to categorize the unfiltered data into 3 classes, with each class corresponding to a different molecular configuration through which an electron can travel:

i. Class 1 - no molecule between the electrodes (quantum tunneling)

ii. Class 2 - single-molecule transport via benzene rings of OPE3

iii. Class 3 - single-molecule transport via Au-S bonds of OPE3

It is important to note that although these classifications are specific to the OPE3 molecule, similar classifications can be made for other complex molecules that can be placed within a mechanically-controlled break junction.

Unsupervised machine learning was used to divide the experimental data into the classes representing the transport channels. First, a clustering algorithm known as the K-means++

method took graphical representations of the data and classified them based on the shape of the 2D histograms. Then, principal component analysis (PCA) is used to obtain a reduced representation of the high-dimensional space while preserving the maximum data variance.

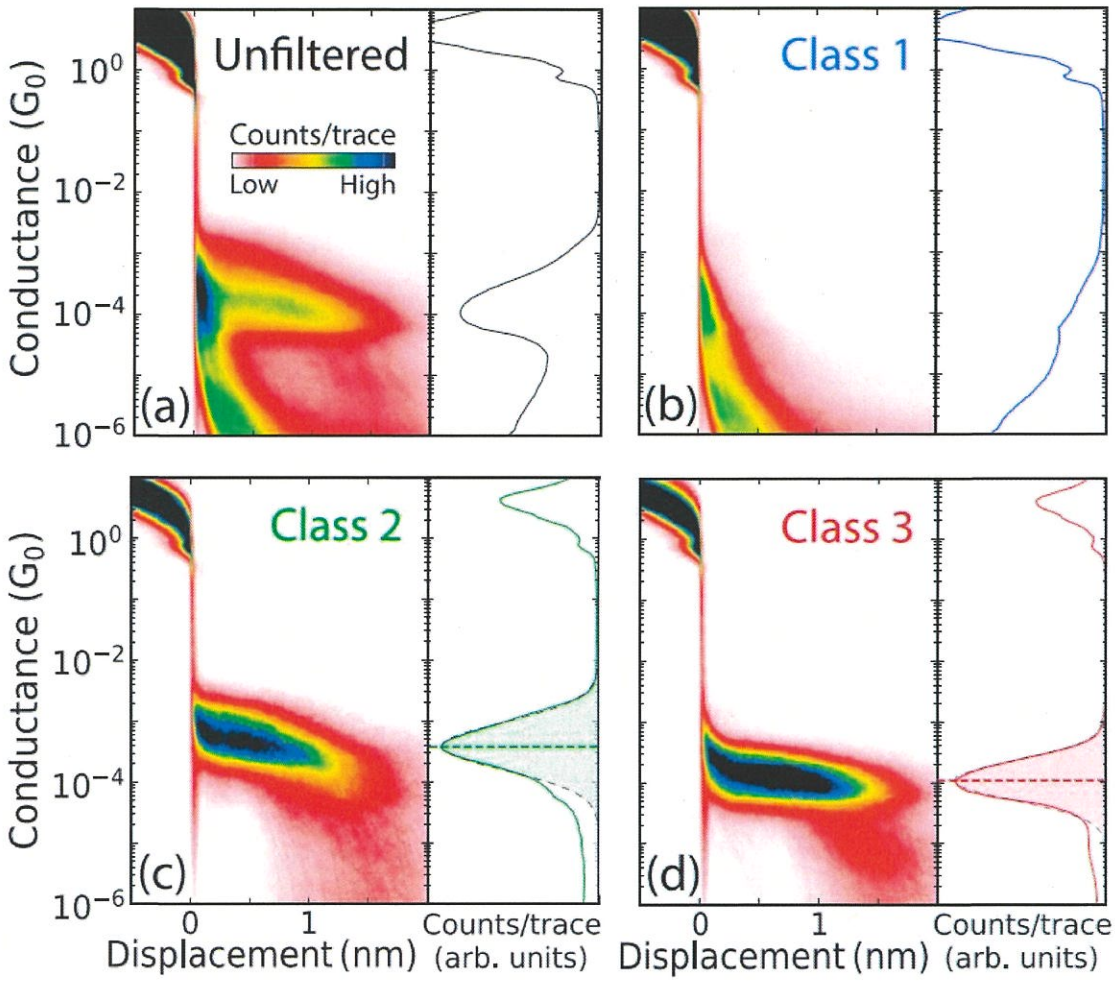

Figure 5: The results of the study by Cabosart et al. A) Includes all of the raw data. B) Includes points attributed to background tunneling. C) Includes data attributed to transport via benzene rings. D) Includes data attributed to transport via Au-S bonds. Source: Adapted from Cabosart et al.

Mathematical Model

Assuming ε and Γ are independent random variables, the probability density function of the conductance g (in units of $G_0 = 2e^2/h$) is:

$$\mathscr{P}_{\mathrm{NR}}(g) \propto \int_{-\infty}^{\infty} \mathrm{d}\varepsilon \int_{0}^{\infty} \mathrm{d}\Gamma \mathscr{P}_{\varepsilon}(\varepsilon)\mathscr{P}_{\Gamma}(\Gamma)\delta[g - T_{\mathrm{NR}}(E_{\mathrm{F}})]$$

Further assuming that ε and Γ are normally distributed, we get

$$\mathscr{P}_{NR}(g) \propto \frac{1}{\sqrt{g(1-g)^3}} \exp\left[-\frac{(c_\varepsilon\sqrt{g} - c_\Gamma\sqrt{1-g})^2}{2(1-g)} \right]$$

where $c_\varepsilon = |E_F - \tilde{\varepsilon}|/\delta_\varepsilon$ and $c_\Gamma = \Gamma/\delta_\Gamma$. The above model describes a probability density function for a symmetric nonresonant break junction, however it does not take into account the effect that background tunneling has on the system, which cannot be ignored.

Background tunneling can be modeled as an energy barrier of height V and spatial width w. The transmission probability function for background tunneling can then be represented as

$$T_{background}(E) \approx \frac{16E}{V} \exp\left[-2\frac{\sqrt{2mV}}{\hbar} w \right]$$

The conductance probability function can then be represented as

$$\mathscr{P}_{background}(g) \propto \int_0^\infty dV \int_0^\infty dw \mathscr{P}_V(V)\mathscr{P}_w(w)\delta[g - T_{background}(E_F)]$$

Assuming w and V are distributed uniformly and log-normally, respectively, we can simplify the conductance probability function to get

$$\mathscr{P}_{background}(g) \propto \frac{\Theta(g - g_-)}{g}$$

where g_- is the threshold conductance. The threshold conductance is the minimum conductance required so that background tunneling actually occurs. Normally, this value is very small. This is placed inside a Heaviside step function because when g is less than g_-, the Heaviside step

function outputs 0, therefore there is no probability that the electron will transmit at that conductance. This function, then, can be approximated as just an exponential decay.

Computational Model

I built a Python program to run simulations using the MolStat package to find the best fit of the mathematical model to experimental data. MolStat contains methods which, given a mathematical model and guesses for the constants in the model, finds a fit for the data. My Python program takes an initial guess for the constants c_ε , c_Γ , and $g_.$. Then, it generates model lines using the probability density functions of g for both non-resonant and background channels. It iterates over thousands of other guesses in search of the smallest residual values between the model and experimental lines. Finally, the "line of best fit" is found when convergence is achieved and the program exits. Matplotlib is then used to visualize the output of the computational model and compare them with the experimental data in graphical form.

V. Results

For the unfiltered data, which represents all of the data taken from the break junction, the value obtained for C_ε was 175.85, the value obtained for C_Γ was 2.5631, the value obtained for $G_.$ was $4.2540 * 10^{-7} G_0$, and the residual value was 1.727592. An excellent fit was produced for the experimental data. Without taking background tunneling into account, the tails of the graph would not have been tracked well. For class 1, which represented the background quantum tunneling, an exponential decay was used to approximate the data, so no values of the constants were produced. For class 2, which represented the electron transport through the benzene rings of OPE3, the value obtained for C_ε was 132.21, the value obtained for C_Γ was 2.9438, the value

obtained for $G_{.}$ was 1.2897 * 10^{-6} G_0, and the residual value was 3.013133. A good fit was produced for this class as well. For class 3, which represented electron transport through Au-S bonds in the OPE3 molecule, the value obtained for C_{ε} was 306.20, the value obtained for C_{Γ} was 3.4331, the value obtained for $G_{.}$ was 2.7401 * 10^{-7} G_0, and the residual value was 4.169986. A good fit was produced for this class of data.

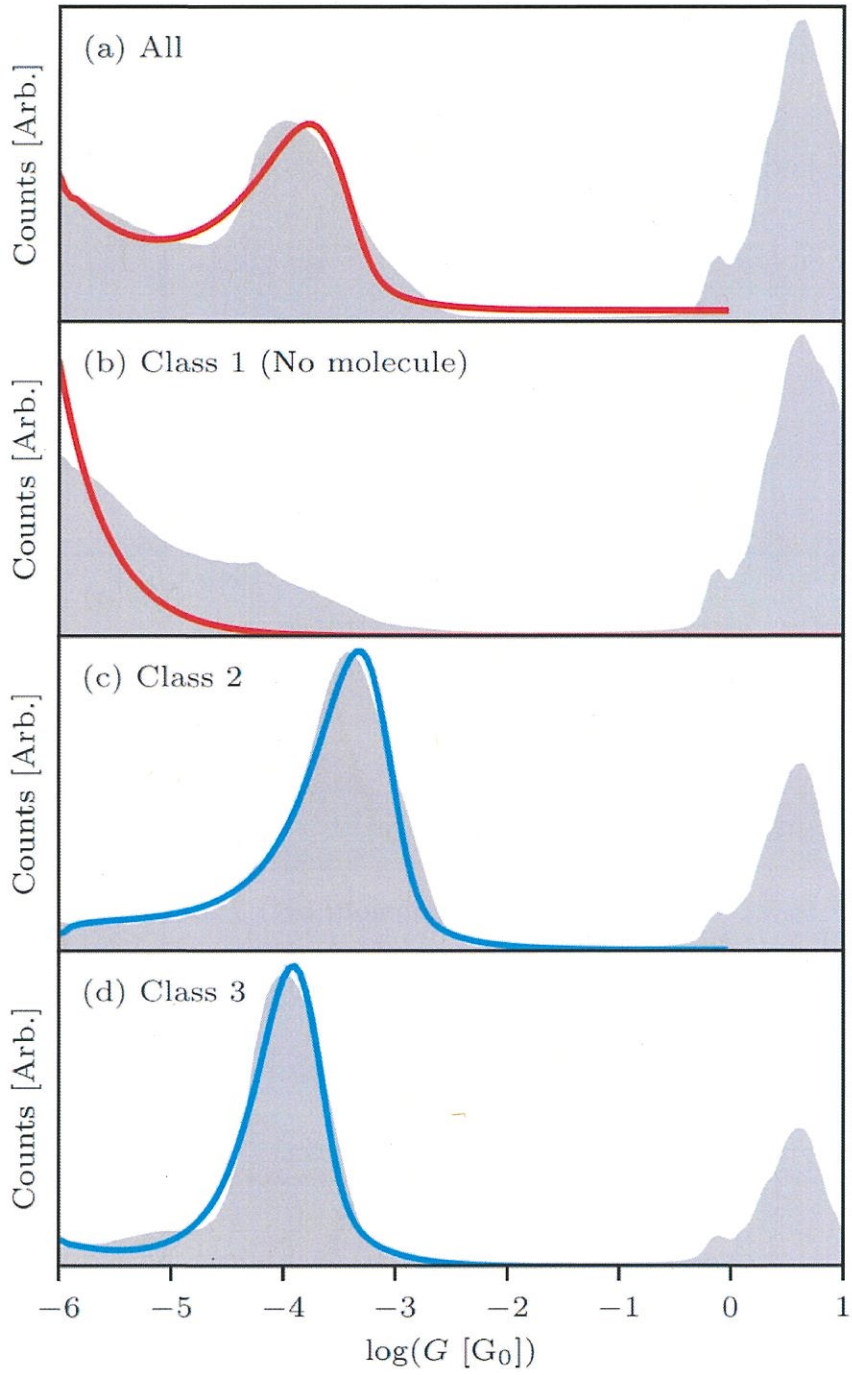

Figure 6: Depicts the experimental data vs. the fit produced by the mathematical model for a) the unfiltered data, b) the results due to background tunneling, c) the results due to transport via benzene rings, and d) the results due to transport via Au-S bonds. All classes of data are well predicted by the mathematical model, showing that each class acts independently of one another. Source: Student generated data.

VI. Discussion

Machine learning techniques were successfully able to classify the experimental data into three unique classes in OPE3: background tunneling, benzene rings, and Au-S bonds. These same techniques can be used to identify the unique channels of electron transport for different molecules in mechanically-controlled break junctions. The mathematical model created in our research which accounts for background tunneling successfully fits to unfiltered data and classes 2 and 3. The model for the unfiltered data would not have tracked the tail as well without the effects of background tunneling taken into effect. In each graph, a peak began at approximately 1 G_0. This peak can be ignored as these correspond to electron transport occurring before the electrodes are fully pulled apart from one another. If background tunneling effects were ignored, the model outputs would be off of the experimental data by approximately 25%. Class 1 was fitted to 1/G to approximate the tunneling effect. It is clear that Class 2, which includes travel over the benzene rings of OPE3, was the most efficient, so devices that make use of OPE3 should be optimized to favor electron transport through the benzene rings of the molecule. Since the mathematical model matches both the unfiltered data and the classified data, it confirms that the machine learning algorithm used to classify the data is correct.

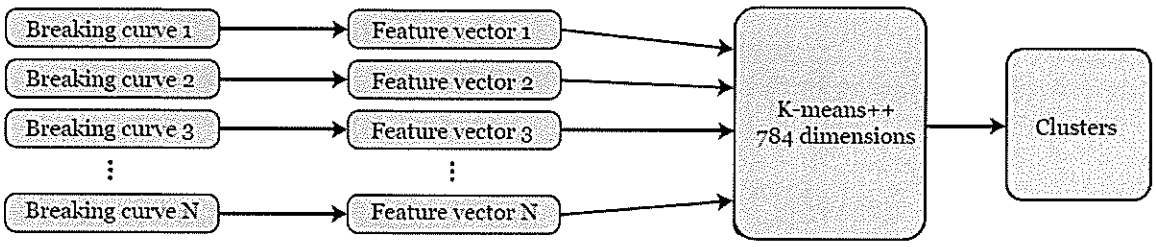

Figure 10: Schematic of the machine learning clustering algorithm used to classify the experimental data. Source: student generated image

VII. Conclusion

We developed a physical and computational model that can analyze conductance histograms and extract electronic properties of a molecule. These properties include the predominant channel's energy and the coupling strength to the electrodes. Quantum tunneling also plays a significant role in single-molecule conductance, as it improved the model by approximately 25%. The machine learning algorithm used to classify the experimental data into 3 categories representing the method of electron transport can be used to classify other molecules into different transport channels. This should create distinct classes that are able to be tracked by the mathematical model as well as the unfiltered data, just as what happened in the OPE3 molecule.

Many applications exist in the fields of electron transport and break junction research. By studying OPE3, we can improve the efficiency of solar cells built with OPE3 molecules. OPE3 is used in polymer form in carbon-based photovoltaics, so understanding how electrons flow through this molecule is critical to designing more efficient solar cells. Break junctions also have applications in detecting cancer biomarkers like Epidermal Growth Factor Receptor. Lastly, break junctions can help to improve the reproducibility of single-molecule transistors.

VIII. Future Work

There is a plethora of future research topics to explore in the field of electron transport. Although we have built a model for symmetrical break junctions, we do not currently have a way of predicting a probability density function for asymmetrical break junctions, where there are different electrodes therefore $\Gamma_L \neq \Gamma_R$. Creating a model for this would allow us to model more

realistic systems more accurately, as usually, both electrodes are not identical. Another future research endeavor would be to study multi-molecule break junctions. In these break junctions, cooperative effects between the molecules cannot be ignored, so modeling the cooperative effects would provide insight into how electron transport is affected by multiple molecules [23].

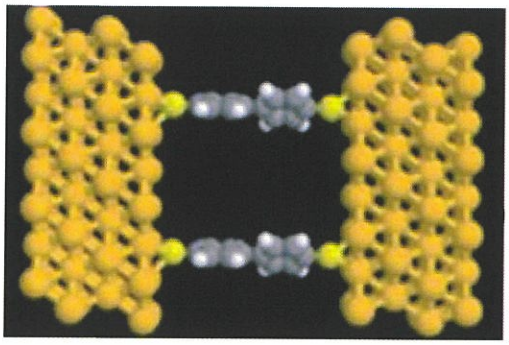

Figure 11: Break junction depicting multiple molecules within the gap. Cooperative effects would have to be taken into account to successfully create a model to represent this type of system. Source: Adapted from Reuter et al.

In the future, research could also be done to improve the accuracy of the mathematical and computational model created by applying it to experimental data extracted from break junctions with different molecules and electrodes. Lastly, future researchers can study the resonant cases where the multiple pathways through the molecule exist and quantum interferences may lead to other interesting behavior.

IX. References

[1] Agraït, N. "Quantum Properties of Atomic-Sized Conductors." *Physics Reports*, vol. 377, no. 2-3, 2003, pp. 81–279., doi:10.1016/s0370-1573(02)00633-6.

[2] Andrews, David Q., et al. "Stochastic Modulation in Molecular Electronic Transport Junctions: Molecular Dynamics Coupled with Charge Transport Calculations." *Nano Letters*, vol. 8, no. 4, 2008, pp. 1120–1126., doi:10.1021/nl0732651.

[3] Aradhya, Sriharsha V., et al. "Dissecting Contact Mechanics from Quantum Interference in Single-Molecule Junctions of Stilbene Derivatives." *Nano Letters*, vol. 12, no. 3, 2012, pp. 1643–1647., doi:10.1021/nl2045815.

[4] Bergfield, Justin P., et al. "The Number of Transmission Channels Through a Single-Molecule Junction." *ACS Nano*, vol. 5, no. 4, 2011, pp. 2707–2714., doi:10.1021/nn1030753.

[5] Büttiker, M., et al. "Generalized Many-Channel Conductance Formula with Application to Small Rings." *Physical Review B*, vol. 31, no. 10, 1985, pp. 6207–6215., doi:10.1103/physrevb.31.6207.

[6] Cabosart, Damien, et al. "A Reference-Free Clustering Method for the Analysis of Molecular Break-Junction Measurements." *Applied Physics Letters*, vol. 114, no. 14, 2019, p. 143102., doi:10.1063/1.5089198.

[7] Cuevas, Juan Carlos, and Elke Scheer. "Molecular Electronics." *World Scientific Series in Nanoscience and Nanotechnology*, 2017, doi:10.1142/10598.

[8] French, William R., et al. "Structural Origins of Conductance Fluctuations in Gold–Thiolate Molecular Transport Junctions." *The Journal of Physical Chemistry Letters*, vol. 4, no. 6, 2013, pp. 887–891., doi:10.1021/jz4001104.

[9] Frisenda, R., and H. S. J. Van Der Zant. "Transition from Strong to Weak Electronic Coupling in a Single-Molecule Junction." *Physical Review Letters*, vol. 117, no. 12, 2016, doi:10.1103/physrevlett.117.126804.

[10] Frisenda, Riccardo, et al. "Statistical Analysis of Single-Molecule Breaking Traces." *Physica Status Solidi (b)*, vol. 250, no. 11, 2013, pp. 2431–2436., doi:10.1002/pssb.201349236.

[11] Ghahramani, Saeed. *Fundamentals of Probability*. Prentice Hall, 2000.

[12] Gotsmann, B., et al. "Direct Electrode-Electrode Tunneling in Break-Junction Measurements of Molecular Conductance." *Physical Review B*, vol. 84, no. 20, 2011, doi:10.1103/physrevb.84.205408.

[13] Guédon, Constant M., et al. "Observation of Quantum Interference in Molecular Charge Transport." *Nature Nanotechnology*, vol. 7, no. 5, 2012, pp. 305–309., doi:10.1038/nnano.2012.37.

[14] Hamill, J. M., et al. "Fast Data Sorting with Modified Principal Component Analysis to Distinguish Unique Single Molecular Break Junction Trajectories." *Physical Review Letters*, vol. 120, no. 1, 2018, doi:10.1103/physrevlett.120.016601.

[15] Inkpen, Michael S., et al. "New Insights into Single-Molecule Junctions Using a Robust, Unsupervised Approach to Data Collection and Analysis." *Journal of the American Chemical Society*, vol. 137, no. 31, 2015, pp. 9971–9981., doi:10.1021/jacs.5b05693.

[16] Lemmer, Mario, et al. "Unsupervised Vector-Based Classification of Single-Molecule Charge Transport Data." *Nature Communications*, vol. 7, no. 1, 2016, doi:10.1038/ncomms12922.

[17] Natelson, Douglas. "Mechanical Break Junctions: Enormous Information in a Nanoscale Package." *ACS Nano*, vol. 6, no. 4, 2012, pp. 2871–2876., doi:10.1021/nn301323u.

[18] Nitzan, A. "Electron Transport in Molecular Wire Junctions." *Science*, vol. 300, no. 5624, 2003, pp. 1384–1389., doi:10.1126/science.1081572.

[19] Paulsson, Magnus, et al. "Conductance of Alkanedithiol Single-Molecule Junctions: A Molecular Dynamics Study." *Nano Letters*, vol. 9, no. 1, 2009, pp. 117–121., doi:10.1021/nl802643h.

[20] Perrin, Mickael L., et al. "Influence of the Chemical Structure on the Stability and Conductance of Porphyrin Single-Molecule Junctions." *Angewandte Chemie*, vol. 123, no. 47, 2011, pp. 11419–11422., doi:10.1002/ange.201104757.

[21] Perrin, Mickael L., et al. "Large Tunable Image-Charge Effects in Single-Molecule Junctions." *Nature Nanotechnology*, vol. 8, no. 4, 2013, pp. 282–287., doi:10.1038/nnano.2013.26.

[22] Quan, Robert, et al. "Quantitative Interpretations of Break Junction Conductance Histograms in Molecular Electron Transport." *ACS Nano*, vol. 9, no. 7, 2015, pp. 7704–7713., doi:10.1021/acsnano.5b03183.

[23] Reuter, Matthew G., et al. "Signatures of Cooperative Effects and Transport Mechanisms in Conductance Histograms." *Nano Letters*, vol. 12, no. 5, 2012, pp. 2243–2248., doi:10.1021/nl204379j.

[24] Reuter, Matthew. "MolStat." *Bitbucket*, 2019, bitbucket.org/mgreuter/molstat.

[25] Schwarz, Florian, and Emanuel Lörtscher. "Break-Junctions for Investigating Transport at the Molecular Scale." *Journal of Physics: Condensed Matter*, vol. 26, no. 47, 2014, p. 474201., doi:10.1088/0953-8984/26/47/474201.

[26] Smit, R. H. M., et al. "Measurement of the Conductance of a Hydrogen Molecule." *Nature*, vol. 419, no. 6910, 2002, pp. 906–909., doi:10.1038/nature01103.

[27] Stefani, Davide, et al. "Large Conductance Variations in a Mechanosensitive Single-Molecule Junction." *Nano Letters*, vol. 18, no. 9, 2018, pp. 5981–5988., doi:10.1021/acs.nanolett.8b02810.

[28] Szyja, Bartłomiej M., et al. "Conformation-Dependent Conductance through a Molecular Break Junction." *Journal of Molecular Modeling*, vol. 19, no. 10, 2013, pp. 4173–4180., doi:10.1007/s00894-013-1794-z.

[29] Taniguchi, Masateru, et al. "Dependence of Single-Molecule Conductance on Molecule Junction Symmetry." *Journal of the American Chemical Society*, vol. 133, no. 30, 2011, pp. 11426–11429., doi:10.1021/ja2033926.

[30] Tschudi, Stephen E, and Matthew G Reuter. "Estimating the Landauer–Büttiker Transmission Function from Single Molecule Break Junction Experiments." *Nanotechnology*, vol. 27, no. 42, 2016, p. 425203., doi:10.1088/0957-4484/27/42/425203.

[31] Valkenier, Hennie, et al. "Cross-Conjugation and Quantum Interference: a General Correlation?" *Phys. Chem. Chem. Phys.*, vol. 16, no. 2, 2014, pp. 653–662., doi:10.1039/c3cp53866d.

[32] Venkataraman, Latha, et al. "Dependence of Single-Molecule Junction Conductance on Molecular Conformation." *Nature*, vol. 442, no. 7105, 2006, pp. 904–907., doi:10.1038/nature05037.

[33] Venkataraman, Latha, et al. "Single-Molecule Circuits with Well-Defined Molecular Conductance." *Nano Letters*, vol. 6, no. 3, 2006, pp. 458–462., doi:10.1021/nl052373+.

[34] Wang, Lu, et al. "Advance of Mechanically Controllable Break Junction for Molecular Electronics." *Molecular-Scale Electronics Topics in Current Chemistry Collections*, 2017, pp. 45–86., doi:10.1007/978-3-030-03305-7_2.

[35] Wang, Ya-Hao, et al. "Conductance Measurement of Carboxylic Acids Binding to Palladium Nanoclusters by Electrochemical Jump-to-Contact STM Break Junction." *Electrochimica Acta*, vol. 123, 2014, pp. 205–210., doi:10.1016/j.electacta.2014.01.041.

[36] Williams, Patrick D., and Matthew G. Reuter. "Level Alignments and Coupling Strengths in Conductance Histograms: The Information Content of a Single Channel Peak." *The Journal of Physical Chemistry C*, vol. 117, no. 11, 2013, pp. 5937–5942., doi:10.1021/jp310180s.

[37] Wu, Ben H., et al. "Uncovering Hierarchical Data Structure in Single Molecule Transport." *The Journal of Chemical Physics*, vol. 146, no. 9, 2017, p. 092321., doi:10.1063/1.4974937.

[38] Xiang, Dong, et al. "Mechanically Controllable Break Junctions for Molecular Electronics." *Advanced Materials*, vol. 25, no. 35, 2013, pp. 4845–4867., doi:10.1002/adma.201301589.

[39] Xu, B. "Measurement of Single-Molecule Resistance by Repeated Formation of Molecular Junctions." *Science*, vol. 301, no. 5637, 2003, pp. 1221–1223., doi:10.1126/science.1087481.

[40] Xu, Bingqian, et al. "Characterizing Molecular Junctions through the Mechanically Controlled Break-Junction Approach." *Reports in Electrochemistry*, 2014, p. 1., doi:10.2147/rie.s46629.

[41] Yanson, A. I., et al. "Formation and Manipulation of a Metallic Wire of Single Gold Atoms." *Nature*, vol. 395, no. 6704, 1998, pp. 783–785., doi:10.1038/27405.

[42] Zhang, Gaibo, et al. "Is Molecular Rectification Caused by Asymmetric Electrode Couplings or by a Molecular Bias Drop?" *The Journal of Physical Chemistry C*, vol. 119, no. 11, 2015, pp. 6254–6260., doi:10.1021/jp5093515.

[43] Zhou, Xiao-Shun, et al. "An Electrochemical Jump-to-Contact STM-Break Junction Approach to Construct Single Molecular Junctions with Different Metallic Electrodes." *Electrochemistry Communications*, vol. 13, no. 5, 2011, pp. 407–410., doi:10.1016/j.elecom.2011.02.005.